# THE EFFECT OF INTER-USER MODELING VARIABILITY ON ANEURYSM PRESSURE AND WALL SHEAR STRESS

ME C213: FINAL PROJECT REPORT

**Bryan Gan, Numi Sveinsson Cepero**

**Student IDs: 3035282394, 3035932340**

**Department of Mechanical Engineering**

**The University of California, Berkeley**

December 2023

## Contents

## List of Figures



## List of Tables

## 1 Introduction

Aortic aneurysms are the second most common disease afflicting the aorta, the largest artery in the body, and the nineteenth most common cause of death overall (Bossone and Eagle, 2021). An aneurysm is defined as a ballooning, or widening, of the vessel wall $\geq 50\%$ than that of a healthy case (Bossone and Eagle, 2021). This widening impacts the blood flow circulation and if left untreated, can lead to rupture causing blood loss and death. Common diagnostic methods include geometric evaluation, eg. diameter measurement, and growth measurement, eg. diameter change over time, to decide if aneurysm needs intervention. Because of aneurysm's effect on hemodynamics, computational modeling has been proposed for diagnosing, understanding disease progression and treatment planning.

Computational modeling of cardiovascular function can provide crucial information regarding how physiological events work. Most commonly, computational cardiovascular modeling involves 3D computational fluid dynamics of blood vessels of interest. This usually involves constructing patient-specific blood vessel geometry from image data such as CT or MRI scans. The geometry is meshed, boundary conditions are set and a set of equations representing the underlying physics phenomena are solved, e.g. the Navier-Stokes equations. See Figure 1 for a typical pipeline for such model construction. The finite element method is most popular for solving the partial differential equations across the domain of interest. The results then contain spatial and temporal distributions of flow values of interest, in our case pressure and velocity. These results can further be used to calculate useful metrics, eg. wall shear stress, indicative for cardiovascular health.

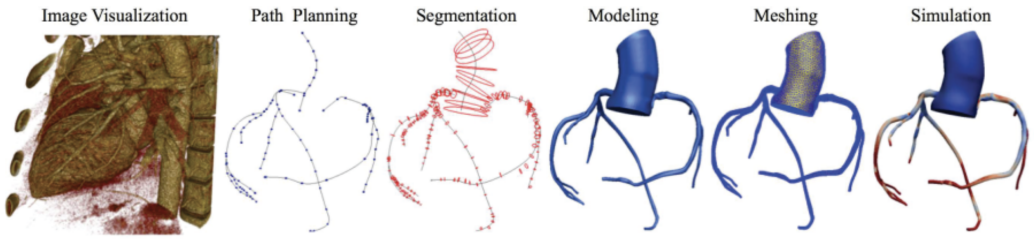


*Fig. 1 The SimVascular image-based modeling pipeline*

Figure 1: A typical patient-specific vascular computational model construction pipeline. Figure borrowed from Simvascular website documentation, `simvascular.com` (Updegrove et al., 2017).

For aneurysm analysis, biomechanical markers such as wall shear stress (WSS), pressure and strain have gained prominent roles for diagnosing and understanding disease progression (Shang et al., 2013) (Guala et al., 2019) (Guzzardi et al., 2015). In particular WSS distribution and WSS derived factors have been linked to aneurysm rupture risk (Zhou et al., 2017). Specifically, wall shear stress is calculated lower in aneurysms than native connected vessels (Shojima et al., 2004). Furthermore, amongst aneurysms, a lower wall shear stress distribution has been linked to increased rupture risk (Zhou et al., 2017). The theory states that stagnant flows in aneurysms lead to low wall shear stress which promotes inflammation of the endothelial cells, which by enzyme release cause degradation of the wall integrity (Cebral et al., 2011). And by breakdown of the wall structure, an aneurysm grows or ruptures. On the other hand, other studies relate areas of high WSS to aneurysm rupture (Zhang et al., 2013). Because of these findings, relating WSS to aneurysm progression and rupture remains an unresolved and controversial subject in the field and has not entered clinical protocols. And this begs the question: how reliable are wall shear stress metrics from patient-specific CFD models, and specifically, how much error is introduced through user dependent modeling techniques?

One of major sources of error in patient-specific computational cardiovascular models of is sourced from geometric modeling. Constructing a three dimensional domain of interest of a blood vessel based on medical images has two main sources of error (see Figure 2):

1. going from human body to medical image scan
2. going from medical image scan to three dimensional model

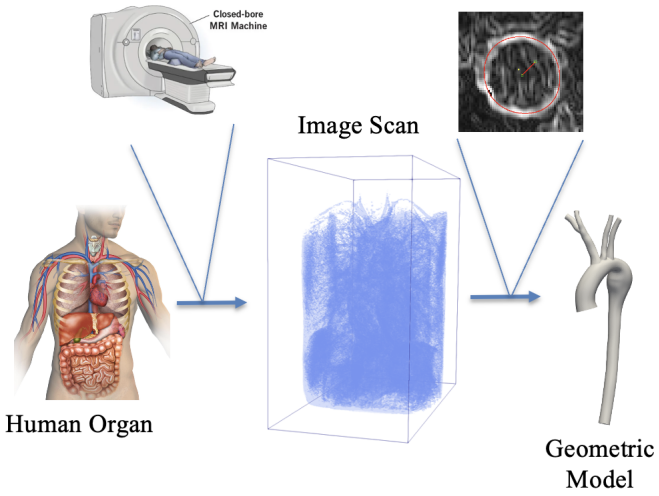


Figure 2: The two sources of error when constructing a patient-specific geometry of patient anatomy using medical image scans. The goal of the project is to estimate the extent and effect of the latter; inter-user modeling variability.

The former refers to how well the imaging technique manages to discern the boundaries of the different tissues in the human body; gradients, resolution and prevalence of image artifacts. The second are human sourced, where a user must directly define where the boundary (in our case, vessel lumen) lies based on the image. This introduces additional variability since different users might make these decisions differently. The goal of this project is to estimate the extent of the latter: how much effect does inter-user variability have on resulting wall shear stress distributions in aortic aneurysms?

To answer this question we perform a study of multiple aortic aneurysm models, each constructed multiple times by different users and resulting computational simulation results of wall shear stress is compared.

## 2 Background

**Marfan syndrome:** Marfan syndrome is a genetic disorder that impacts the body's connective tissue, which plays a crucial role in supporting and structuring all parts of the body. People with Marfan syndrome can experience a range of symptoms due to the effect on various systems, including the skeletal system, eyes, skin, and particularly the cardiovascular system. Serious complications can arise when Marfan syndrome affects the heart and blood vessels, such as the development of an aortic aneurysm.

An aortic aneurysm is a serious condition that occurs when the wall of the aorta, the main artery carrying blood out of the heart, weakens and bulges out. This bulge can become life-threatening if it leads to a dissection, which is a tear in the wall of the aorta that allows blood to leak into the space between the layers of the vessel wall. Both an aneurysm and a dissection can be fatal if not treated promptly and effectively.

By simulating blood flow dynamics specific to a patient's unique vascular geometry, CFD provides detailed insights into shear stresses acting on the vessel walls. This information is valuable for the diagnosis and can help in predicting the growth of aneurysms. In clinical practice, understanding wall shear stress can aid in determining the potential risk of aneurysm formation and progression, which is particularly relevant for Marfan patients due to their susceptibility to such vascular issues.

## 3 Methods

This section outlines the methods of the study. Firstly, the dataset used is explained, then the modeling techniques used and lastly the boundary conditions and other simulation parameters chosen. The software

Simvascular (Updegrove et al., 2017) is used for modeling and simulation purposes and Paraview is used for visualization.

### 3.1 Dataset

Three patients with Marfan syndrome and resulting aortic aneurysms were chosen from Vascular Model Repository, available at vascularmodel.com. The cases chosen are the following:

- nr 22: **0022_H_AO_MFS**
- nr 25: **0025_H_AO_MFS**
- nr 27: **0027_H_AO_MFS**

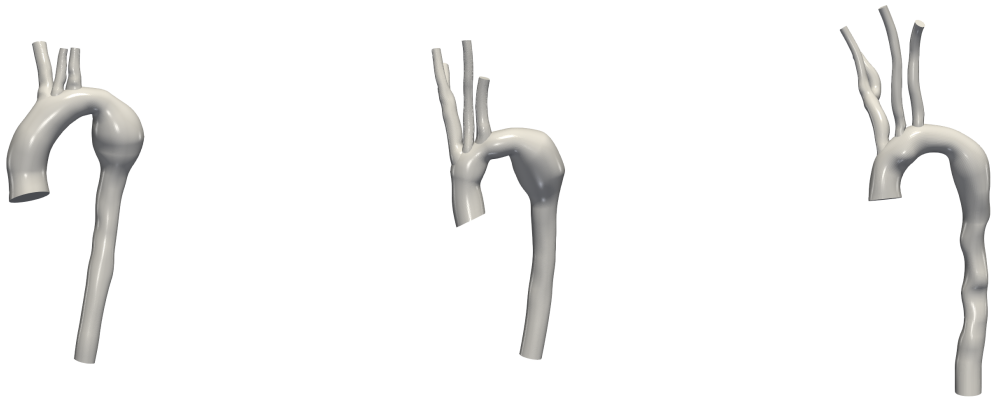

Figure 3: The three cases used for the study. From left: nr 22, 25, and 27. Each one constructed from MRI scans of patients with Marfan syndrome.

Each case has respective MRI scan, surface model and boundary conditions chosen by the original user. To reconstruct the geometric models, the same MRI scan was used for three different 'versions' of the geometry from three different users: the original and two new ones. In total we end up with 9 geometric models, three versions for each of the three cases.

### 3.2 Geometric Modeling

First step involves construction the 3D geometry of the aorta and main aortic branches from the medical image, in this case MRI scan. That involves:

1. Pathline generation: Moving around within the image volume and connecting points to form a 3D spline representing the artery trajection.
2. 2D segmentation: Moving along the pathlines and detailing the extend of the lumen in the cross section.
3. Lofting + Unifying: Lofting the multiple 2D lumen segmentations together into one and unifying all branches into one solid surface model of all connected branches.

See Figure 1 for a diagram with those steps.

The purpose of this study is to explore the differences in geometric modeling of the same anatomic structure by different users. The differences between users may occur from differences in the following decisions:

- Accuracy of pathline. This depends on number of points placed as well as their locations with respect to the center of the vessel. More points are needed along highly curved sections of the vessel for accurate and smooth pathlines.

- Number and placement of 2D segmentations along the pathline. More are needed along curved parts for accurate and smooth three dimensional surface lofting.
- The 2D segmentation method. Methods used ranged from thresholding locally and in batches, using the levelset method, fitting a circle or spline with specific control points, or a mixture of the ones above. These may all results in slightly varying segmentations.

### 3.3 Boundary Conditions

The boundary conditions were as follows:

**Inlet:** Inflow was defined with a time dependent inflow file from the original VMR simulation setup. See the inflow data in Figure 4.

**Outlets:** Each outlet was coupled to the simulation via lumped parameter RCR model relating flow to pressure. The values used are $R_p$: proximal resistance, $C$: capacitance, and $R_d$: distal resistance. Proximal resistance models the resistance of vessel close to outlet and capacitance and distal resistance models the compliance and resistance of the downstream vascular bed. Specific values can be seen in Table 1.

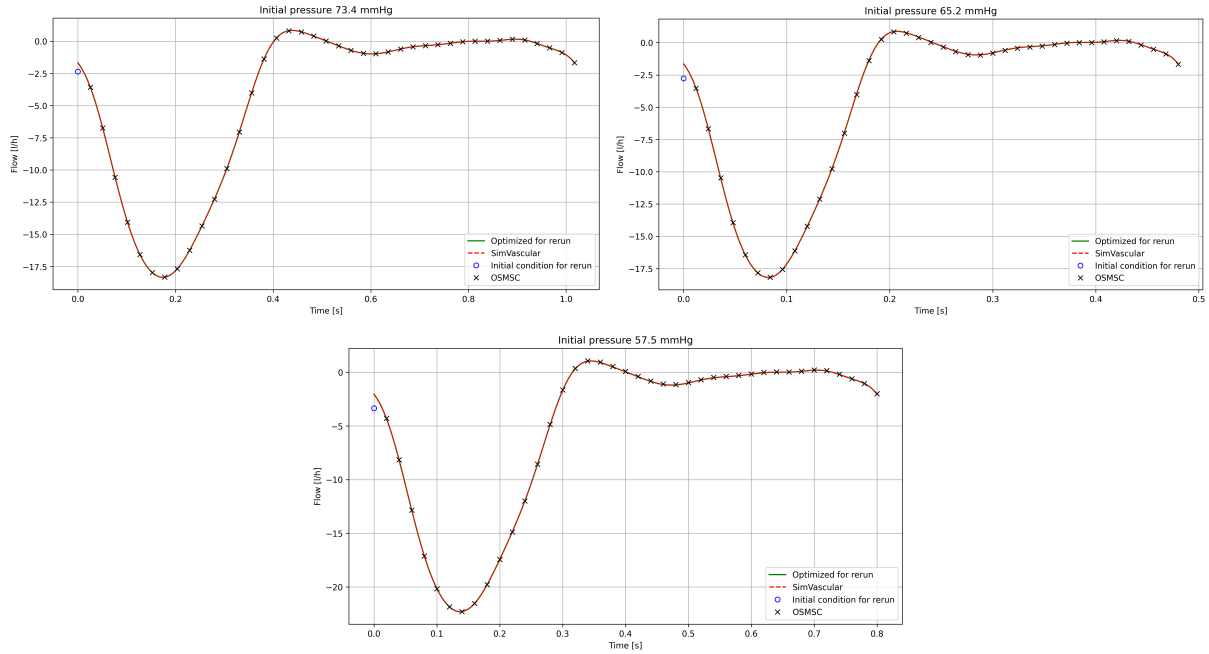


Figure 4: The inflow data used for inlet boundary conditions: top left: 22, top right: 25, bottom: 27. Graphs taken from original Vascular Model Repository projects.

### 3.4 Simulation Parameters

Table 2 shows the values chosen for simulation parameters. A max element size of 0.1 gave global meshes with element count between 1-2 million, and was always smaller than the estimate given by SimVascular Software. A preliminary mesh study was performed and results displayed later in section 4. All simulations are unsteady, rigid wall.

### 3.5 Metrics

For geometric comparison of the models we compute three metrics:

Table 1: The boundary condition values for lumped parameter coupling at outlets. Resistance in unit $\mathrm{dyn} * \mathrm{s}/\mathrm{cm}^5$ and capacitance in unit $\mathrm{cm}^5/\mathrm{dyn}$.

| Case | Branch | $R_p$ | $C$ | $R_d$ |
|---|---|---|---|---|
| 22 | Aorta | 1.52e2 | 2.07e-3 | 1.85e3 |
| | Brachiocephalic Artery | 9.13e2 | 3.46e-4 | 1.12e4 |
| | Left Common Carotid Artery | 2.26e3 | 1.40e-4 | 2.76e4 |
| | Left Subclavian Artery | 1.54e3 | 2.04e-4 | 1.89e4 |
| 25 | Aorta | 2.36e2 | 1.20e-3 | 2.28e3 |
| | Right Subclavian Artery | 7.79e2 | 3.63e-4 | 7.54e3 |
| | Right Common Carotid Artery | 1.31e3 | 2.16e-4 | 1.27e4 |
| | Left Common Carotid Artery | 1.50e3 | 1.89e-4 | 1.45e4 |
| | Left Subclavian Artery | 9.39e2 | 3.01e-4 | 9.06e3 |
| 27 | Aorta | 1.78e2 | 7.82e-4 | 1.71e3 |
| | Right Subclavian Artery | 6.75e2 | 2.04e-4 | 6.44e3 |
| | Right Common Carotid Artery | 1.31e3 | 1.05e-4 | 1.26e4 |
| | Left Common Carotid Artery | 1.12e3 | 1.23e-4 | 1.07e4 |
| | Left Subclavian Artery | 1.01e3 | 1.37e-4 | 9.64e3 |

Table 2: The simulation parameters used.

| Parameter | Value |
|---|---|
| Fluid Viscosity | 0.04 P |
| Fluid Density | 1.06 $\mathrm{g}/\mathrm{ml}$ |
| Max Element Size | 0.01 $\mathrm{cm}$ |
| Time Step Size | 0.001 $\mathrm{s}$ |
| Step Construction | 3 |
| Nr. Timesteps per Cardiac Cycle to Save | 20 |
| Tolerance Momentum Residual | 0.05 |
| Tolerance Conservation Mass Residual | 0.4 |

1. Average Symmetric Surface Distance (ASSD): calculates minimum distances between surfaces and finds the average across all vertices.

2. Hausdorff Distance: calculates the minimum distances between all vertices and finds the maximum of those distances.

3. Volume difference: calculates the volumes of both surfaces and returns the difference.

ASSD gives good insight into overall agreement between the surfaces, Hausdorff gives insight into the severity of outliers, and volumetric difference gives insight into possible bias of 2D segmentations.

For wall shear stress comparison, we isolate the comparison around the aneurysm only since that's the region of interest. Furthermore, we compute the average and maximum wall shear stress on the two sides of the aneurysm, the posterior and anterior sides. This is chosen because of symmetry on other axes. We compute average because of lack of reference frame for the surface meshes, meaning relating specific points on one surface to other ones is difficult, and looking over the average gives more insight rather than point-wise difference.

# 4 Results

## 4.1 Modeling Variability

The resultant geometric models from the three users were compared. Results of a volumetric calculation can be seen in Table 3. Furthermore, we compared the models using three metrics as mentioned above. Those results can be seen in Figure 5. Those results show a volumetric difference of 5-7%, ASSD under 0.03 cm, Hausdorff distance between 0.36-1.61 cm.

Table 3: Geometric models volume

| | Volume [$cm^3$] | | |
|---|---|---|---|
| Case | User 1 | User 2 | User 3 |
| 22 | 150.57 | 141.14 | 151.33 |
| 25 | 115.84 | 109.41 | 114.16 |
| 27 | 111.82 | 112.42 | 125.86 |

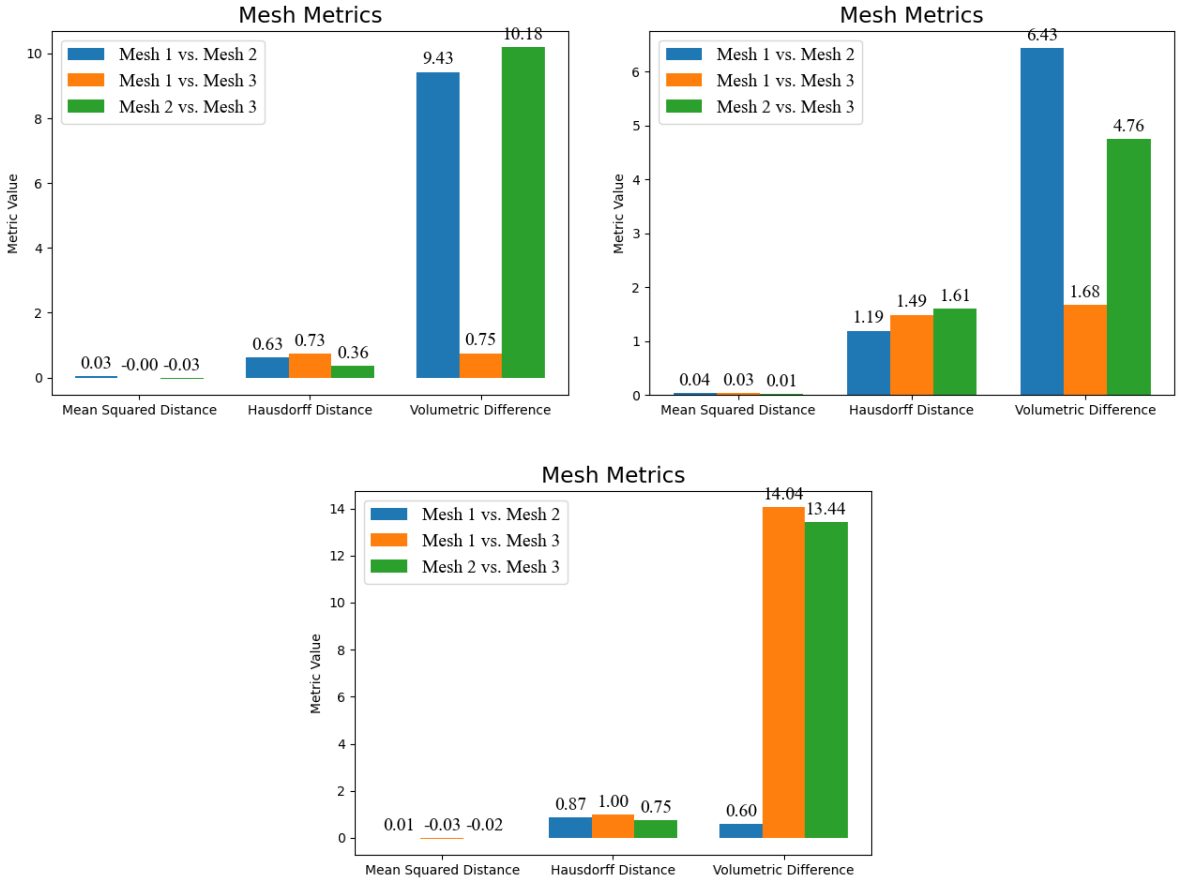


Figure 5: The three cases used for the study. From left: nr 22, 25, and 27. Each one constructed from MRI scans of patients with Marfan syndrome.

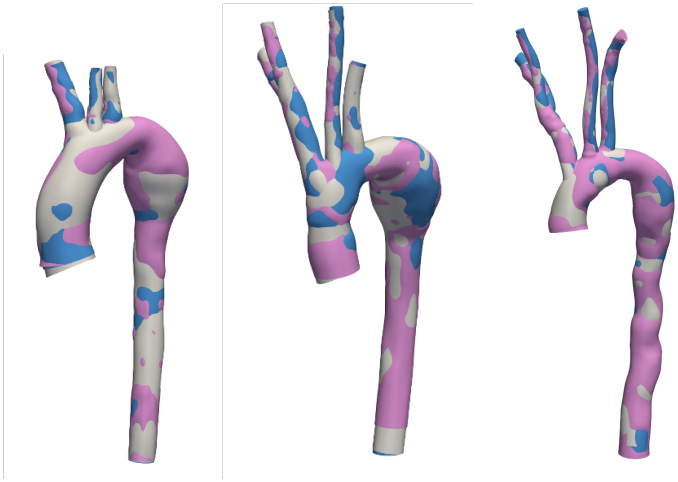

Figure 6: The cases showing the three different surface meshes overlapped on top of each other. From left: 22, 25, 27. White: User 1, Blue: User 2, Pink: User 3.

### 4.2 Aneurysm Wall Shear Stress

We extracted the wall shear stress of the diseased area from simulation results. Using the same boundary planes for each surface, we separately analyzed the results of anterior and posterior aneurysm. See Figure 8-12 for results of surface 22, 25, and 27.

#### 4.2.1 Surface 22

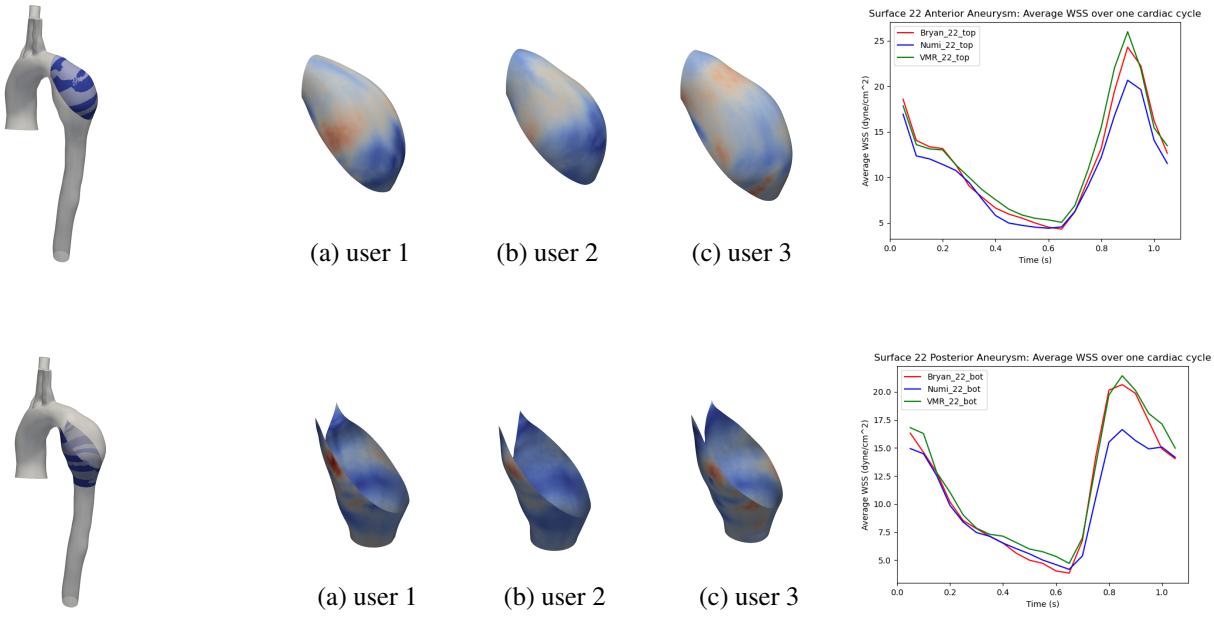


(a) user 1 (b) user 2 (c) user 3

(a) user 1 (b) user 2 (c) user 3

Figure 8: Aneurysm is clipped into anterior and posterior parts using planes that have origin at [-0.5, 1, 1] and normal [0 1 0], origin at [-0.5, 1, 3] and normal [0, 0, -1], and origin at [-3, -1, 6.5] and normal [0 1 -1] and [0 -1 1]. The middle figures show WSS distribution at the timestep where average WSS is the highest. The plots demonstrate the average WSS over one cardiac cycle. Overall, the simulation results of all three users agree with each other, but the maximum value deviates  20 percents.

### 4.2.2 Surface 25

Please see Figure 10 for results.

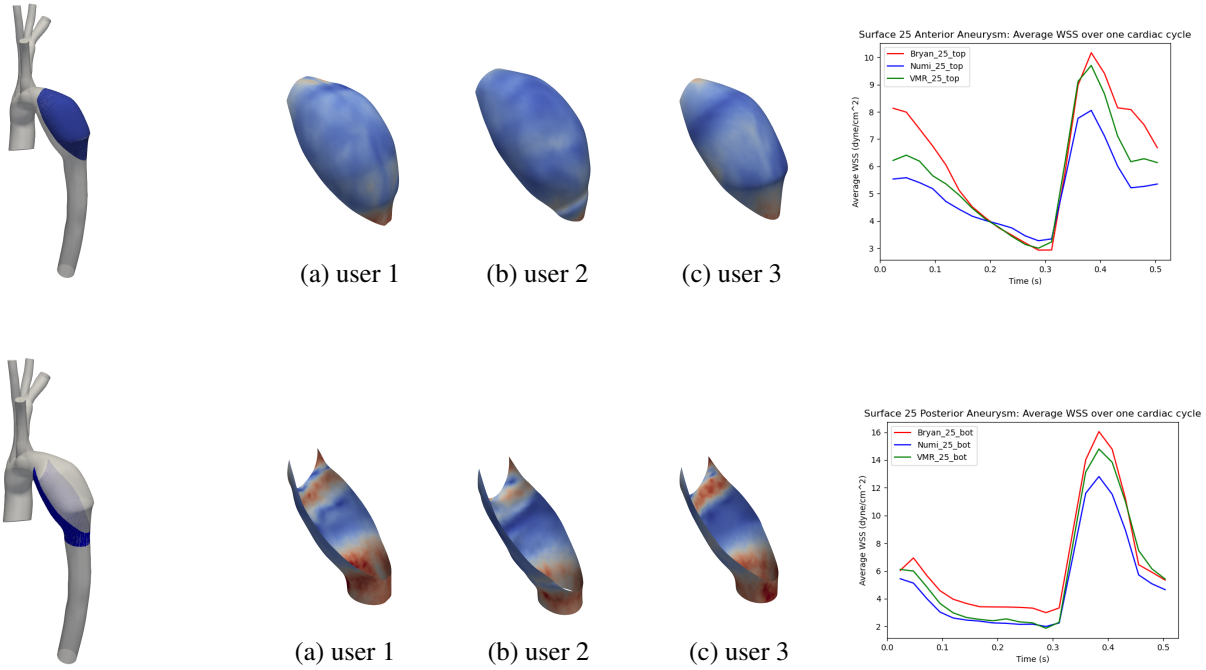


Figure 10: Aneurysm is clipped into anterior and posterior parts using planes that have origin at [-0.5, 1, 1] and normal [0 1 0], origin at [-0.5, 1, -15] and normal [0, 0, -1], and origin at [-3, -1, -11.5] and normal [0 1 -1] and [0 -1 1]. The middle figures show WSS distribution at the timestep where average WSS is the highest. The plots demonstrate the average WSS over one cardiac cycle. Overall, the simulation results of all three users agree with each other, but the maximum value deviates 25 percents.

### 4.2.3 Surface 27

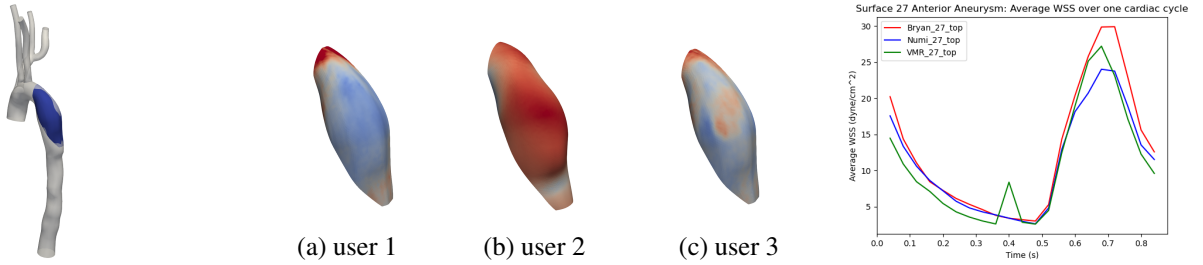


## 4.3 Pressure

We also collected average pressure of the diseased area over one cardiac cycle. We discovered that the computed average pressure over diseased area varies less than 10 percents. Please see Figure 13.

## 4.4 Mesh Study

For verification, we performed a preliminary mesh study to ensure results are converged. To do this we ran the same unsteady simulation for surface 27 with element size 0.08 instead of 0.1. The results can be seen in Figure 14.

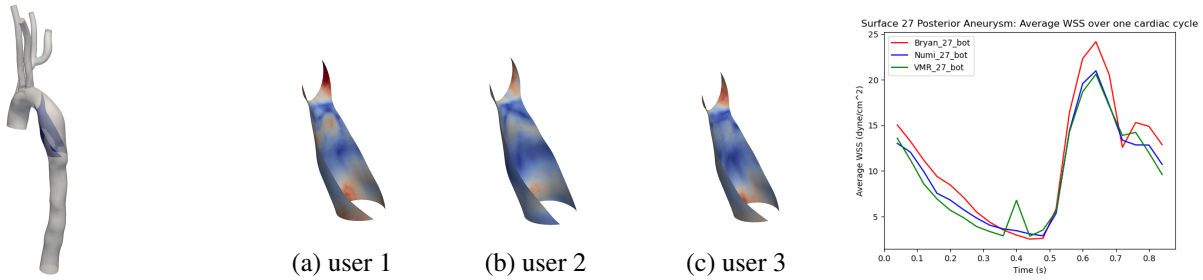


(a) user 1 (b) user 2 (c) user 3

Figure 12: Aneurysm is clipped into anterior and posterior parts using planes that have origin at [0, 1, 1] and normal [0 1 0], origin at [-5, -1, -14] and normal [0, 0, -1], and origin at [-5, 0, -10.5] and normal [0.2 0.8 -0.5] and [-0.2 -0.8 0.5]. The middle figures show WSS distribution at the timestep where average WSS is the highest. The plots demonstrate the average WSS over one cardiac cycle. Overall, the simulation results of all three users agree with each other, but the maximum value deviates 20 percents.

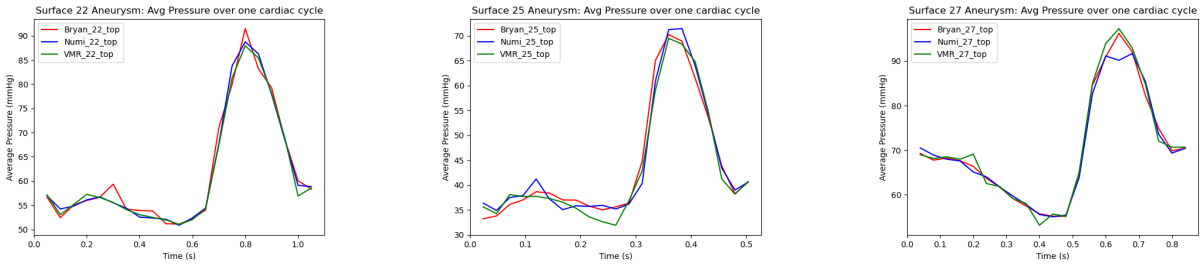


(a) Pressure of surface 22 (b) Pressure of surface 25 (c) Pressure of surface 27

Figure 13: Comparison of average pressure overtime between different users

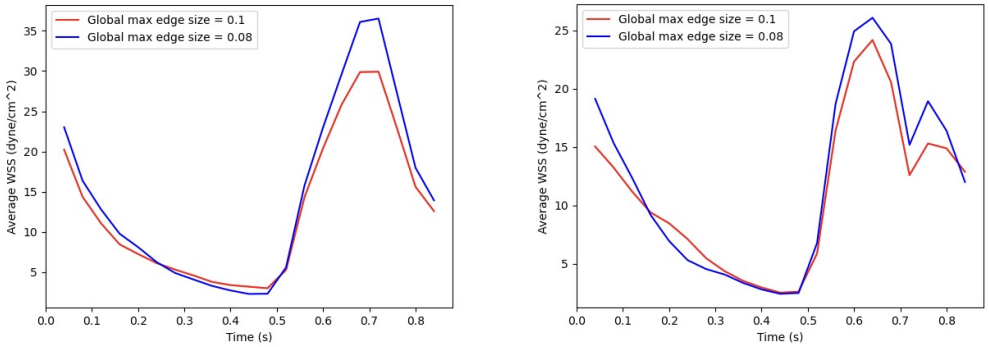


Figure 14: Comparison of average wall shear stress for mesh max element size 0.08 and 0.1. Left: anterior aneurysm, right: posterior aneurysm.

## 5 Discussion and Conclusion

**Findings:** This report investigates the effect of inter-user modeling variability on simulation wall shear stress magnitude and distribution in aortic aneurysms. We analyzed our results and quantified their differences from the aspect of geometric modeling and the aspect of computed wall shear stress in diseased areas.

From the geometric modeling aspect, the surfaces constructed by three different users scored, on average, 0.002 in mean squared distance , 0.959 in Hausdorff distance, and 6.81 in volumetric differences.

From the aspect of computed wall shear stress magnitude and distribution, we conclude that the magnitudes at peak systole vary, on average, 20 percents, while they vary less than 10 percents during diastole.

**Implications:** Our study highlights the significant impact of inter-user variability in geometric modeling on patient-specific simulations for aortic aneurysms. The variations in wall shear stress and pressure due to different modeling techniques underscore the need for caution in using these simulations for clinical decision-making. It's essential to recognize that relying on a single simulation might lead to inaccurate conclusions about disease progression and risk assessment.

This variability points to the necessity of developing standardized guidelines for geometric modeling and considering multiple simulations with varied approaches to get a comprehensive understanding of the patient's condition. Additionally, our study's limitations suggest the importance of larger-scale research and exploring other factors like boundary conditions and fluid properties that might influence simulation outcomes.

In summary, while patient-specific modeling is promising for personalized medicine, it requires comprehensive consideration of modeling variability and parameter standardization to ensure its reliability and effectiveness in clinical applications.

**Limitations:** The main limitations of the study are 1) sample size, 2) focus on modeling effect on simulation results and 3) lack of robust mesh refinement study.

The sample size is only 3 data points, both with regard to number of patients modeled and number of modelers compared over. To get a better estimate of the spread, a bigger sample size is needed.

In the study, we keep all parameters fixed and change the geometric models, however, it is possible that other factors have a much bigger impact on the aneurysm wall shear stress and pressure than the geometric variability. A further study exploring the effect of changing boundary conditions, rigid vs deformable wall, fluid density/viscosity and residual tolerance values on the resulting simulation values is necessary to answer this bigger, and more pressing, question.

Finally, the preliminary mesh refinement study results shows that the solution is possibly not converged. That could mean that the variance we see in aneurysm wall shear stress and pressure could be explained by unconverged solutions. Future work should include a more comprehensive mesh refinement study including possibly lowering time step size to prevent residual blow up.

## References


Adam Updegrove, Nathan M. Wilson, Jameson Merkow, Hongzhi Lan, Alison L. Marsden, and Shawn C. Shadden. SimVascular: An Open Source Pipeline for Cardiovascular Simulation, 3 2017. ISSN 15739686.

Eduardo Bossone and Kim A. Eagle. Epidemiology and management of aortic disease: aortic aneurysms and acute aortic syndromes. *Nature Reviews Cardiology*, 18(5):331–348, May 2021. ISSN 1759-5010. doi:10.1038/s41569-020-00472-6. URL https://doi.org/10.1038/s41569-020-00472-6.

Eric K. Shang, Derek P. Nathan, Shanna R. Sprinkle, Sarah C. Vigmostad, Ronald M. Fairman, Joseph E. Bavaria, Robert C. Gorman, Joseph H. Gorman, Krishnan B. Chandran, and Benjamin M. Jackson. Peak wall stress predicts expansion rate in descending thoracic aortic aneurysms. *The Annals of Thoracic Surgery*, 95(2):593–598, 2013. ISSN 0003-4975. doi:https://doi.org/10.1016/j.athoracsur.2012.10.025. URL https://www.sciencedirect.com/science/article/pii/S0003497512023569.

Andrea Guala, Gisela Teixidó-Tura, Jose Rodríguez-Palomares, Aroa Ruiz-Muñoz, Lydia Dux-Santoy, Nicolas Villalva, Chiara Granato, Laura Galian, Laura Gutiérrez, Teresa González-Alujas, Violeta Sanchez, Alberto Forteza, David García-Dorado, and Artur Evangelista. Proximal aorta longitudinal strain predicts aortic root dilation rate and aortic events in Marfan syndrome. *European Heart Journal*, 40(25):2047–2055, 04 2019. ISSN 0195-668X. doi:10.1093/eurheartj/ehz191. URL https://doi.org/10.1093/eurheartj/ehz191.

David G. Guzzardi, Alex J. Barker, Pim van Ooij, S. Chris Malaisrie, Jyothy J. Puthumana, Darrell D. Belke, Holly E.M. Mewhort, Daniyil A. Svystonyuk, Sean Kang, Subodh Verma, Jeremy Collins, James Carr, Robert O. Bonow, Michael Markl, James D. Thomas, Patrick M. McCarthy, and Paul W.M. Fedak. Valve-related hemodynamics mediate human bicuspid aortopathy. *Journal of the American College of Cardiology*, 66(8):892–900, 2015. doi:10.1016/j.jacc.2015.06.1310. URL https://www.jacc.org/doi/abs/10.1016/j.jacc.2015.06.1310.

Geng Zhou, Yueqi Zhu, Yanling Yin, Ming Su, and Minghua Li. Association of wall shear stress with intracranial aneurysm rupture: systematic review and meta-analysis. *Scientific Reports*, 7(1):5331, Jul 2017. ISSN 2045-2322. doi:10.1038/s41598-017-05886-w. URL https://doi.org/10.1038/s41598-017-05886-w.

Masaaki Shojima, Marie Oshima, Kiyoshi Takagi, Ryo Torii, Motoharu Hayakawa, Kazuhiro Katada, Akio Morita, and Takaaki Kirino. Magnitude and role of wall shear stress on cerebral aneurysm: computational fluid dynamic study of 20 middle cerebral artery aneurysms. *Stroke*, 35(11):2500–2505, November 2004.

J.R. Cebral, F. Mut, J. Weir, and C.M. Putman. Association of hemodynamic characteristics and cerebral aneurysm rupture. *American Journal of Neuroradiology*, 32(2):264–270, 2011. ISSN 0195-6108. doi:10.3174/ajnr.A2274. URL https://www.ajnr.org/content/32/2/264.

Y. Zhang, H. Takao, Y. Murayama, and Y. Qian. Propose a wall shear stress divergence to estimate the risks of intracranial aneurysm rupture. *The Scientific World Journal*, 2013:508131, Sep 2013. ISSN 2356-6140. doi:10.1155/2013/508131. URL https://doi.org/10.1155/2013/508131.